ISSN 0970-5953

Volume 37. No. 4

October - December 2021

PHYSICS EDUCATION

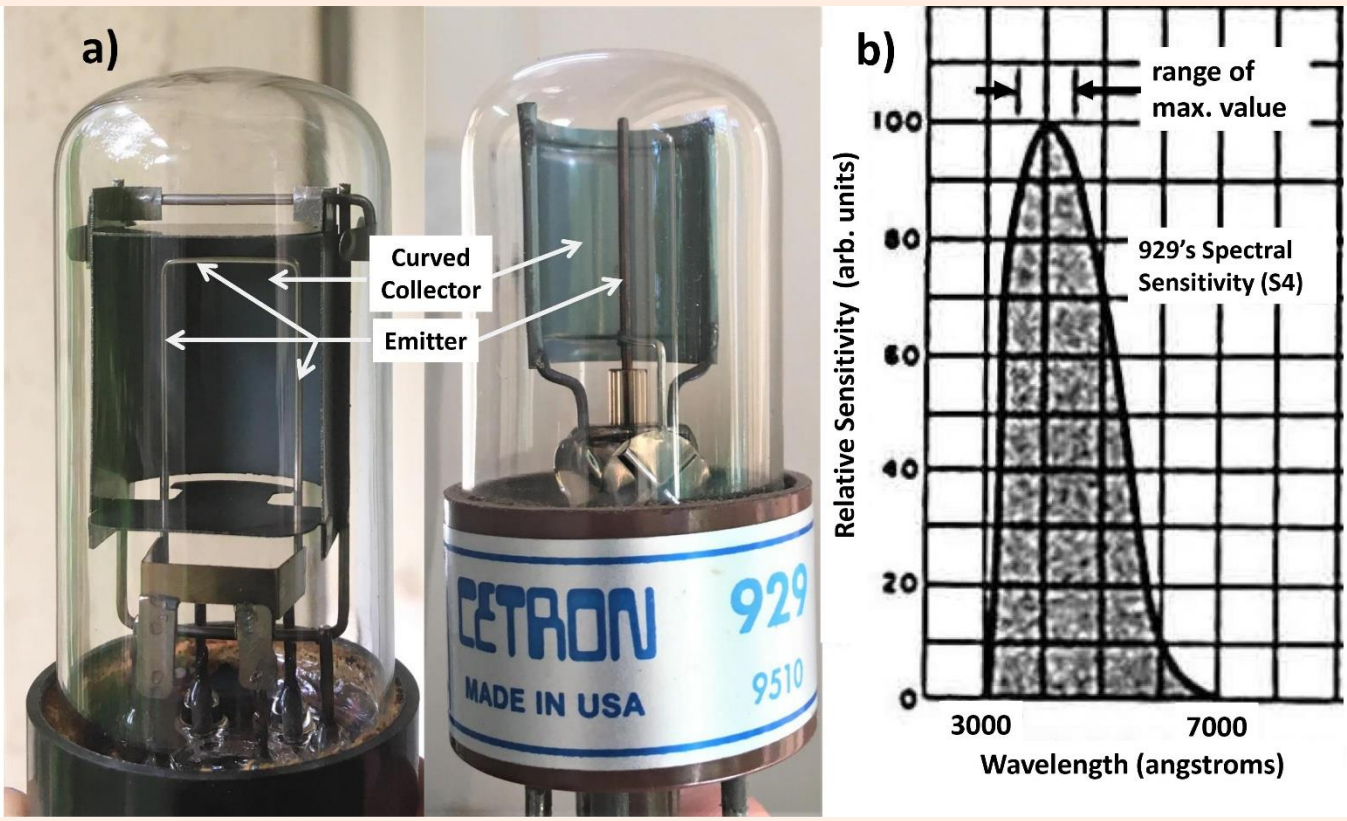

www.physedu.in

Volume 37, Number 4

In this Issue

- **Understanding Monte Carlo Algorithm and its application to a Bose-Einstein System** 13 Pages

  Pragati Ashdhir, Yash Saxena, Adesh Kushwaha and Karun Gadge

- **New and simple method for the determination of critical damping resistance of moving coil galvanometer** 07 Pages

  Bhakta Kunwar

- **Novel method for determination of contact angle of highly volatile liquids** 11 Pages

  K Nilavarasi and V Madhurima

- **Advances and challenges in VLSI designs for nanotechnology** 09 Pages

  Amit Kumar

- **A critical look at the photoelectric effect experiment: a detailed guide for an undergraduate instructor** 26 Pages

  Ashwin Mohan

- **Design and Implementation of e-CALLISTO Tower Mounted LNA using MMIC** 11 Pages

  Dnyandev B. Patil and Vijay S. Kale

Understanding Monte Carlo Algorithm and its application to a Bose-Einstein System

Pragati Ashdhir[1], Yash Saxena[2], Adesh Kushwaha[3] and Karun Gadge[4]

[1]Department of Physics, Hindu College, University of Delhi,Delhi, India.
[2]Department of Physics and Astrophysics, University of Delhi, Delhi, India.
[3]Department of Physics, Indian Institute of Technology Gandhinagar, India.
[4]School of Basic Sciences, Indian Institute of Technology Mandi, India.

1.pragatiashdhir@hinducollege.ac.in
2.1980234@pg.du.ac.in
3.adesh.kushwaha@iitgn.ac.in
4.v19090@students.iitmandi.ac.in

Submitted on 10-05-2021

Abstract

In this paper we study the Monte Carlo Algorithm using two different sampling methods, namely, Direct sampling and Markov chain sampling. In the Markov chain sampling method, Metropolis algorithm is used.

The paper explains the Monte Carlo algorithm and the different sampling approaches in a simplified manner. In connection with this we explore the theory of evaluation of integrals and Hamiltonians. To further clarify the tools, a problem of Boson Gas under a harmonic potential trap is chosen and solved using the Monte Carlo Method. The results obtained using different approaches are compared and presented in the form of plots. The aim of this exercise is to efficiently deliver the concept of Monte Carlo method to the graduate and post-graduate physics students and aid in enhancing their computational skills.

1 Introduction and Background

Today, computational methods are an integral part of problem solving in the varied fields of Theoretical Physics Research. One such powerful computational method is the Monte Carlo Algorithm method. The scope of Monte Carlo method [1] is humongous and a complete presentation of the same in a paper like this cannot be justified. Nevertheless, we have attempted to present a simplified usage of the method for students to understand how to implement it and equip

them to develop it further to solve more complicated problems of contemporary research.

At its core, the Monte Carlo method is a statistical approach to computing integrals. It is a numerical technique that uses random numbers and statistical probability to solve problems where there is absence of analytic solutions due to a large number of entities being present (like the system of real gases) or there exist very complex interactions amongst them. This method of random sampling generally provides reliable approximate solutions. When we look back in history, the first article 'The Monte Carlo Method' by Metropolis and Ulam was published in 1949. It is named after the city of Monte Carlo in Monaco, which is famous for all kinds of gambling.

Markov chain Monte Carlo and Metropolis Algorithm[1]: In the year 1906, Andrey Markov first introduced the Markov chain as a stochastic process(containing random variables whose transition depends upon certain assumptions). *The main idea behind the Markov chain is that the next step of the random variable depends upon the current state only, that is, it's a memory-less process where future action depends on the current action.* For general stochastic simulation techniques known as Markov Chain Monte Carlo, the Metropolis [2] is one of the many algorithms for constructing chains.

In Section A, we have introduced the concepts of different samplings to the reader. After that we have explained the use of these sampling methods in computation of integrals.

In section B, we have chosen a physical problem of Boson gas under a 1-Dimensional Harmonic Potential and have used the concept of Monte Carlo sampling both by Direct method and Markov Chain to estimate the energy eigenvalue for the ground state. The computed energy values are then compared with the exact value obtained by analytical methods.

2 Section A

2.1 What is Sampling?

Sampling is a process where the set of entities is collected from a larger set. Each entity has an equal probability of being picked randomly. Next, we need to understand the two fundamentally different sampling approaches: Direct Sampling and Markov Chain Sampling.

2.2 Direct Sampling:

To understand direct sampling [3] we take up the problem of estimating the value of the constant π.

2.2.1 Motivation and Simple Example: Estimating π

Suppose we have a **square** dartboard and a novice is made to randomly throw darts across the board. After a large number of hits, we inscribe a circle inside the dartboard

as shown in Fig. (1) and calculate the ratio between the number of hits inside the circle to that inside the square.

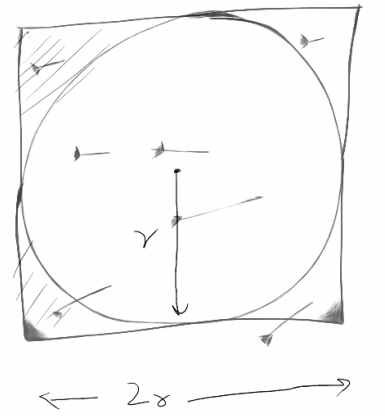

Figure 1: Darts Game for π estimation

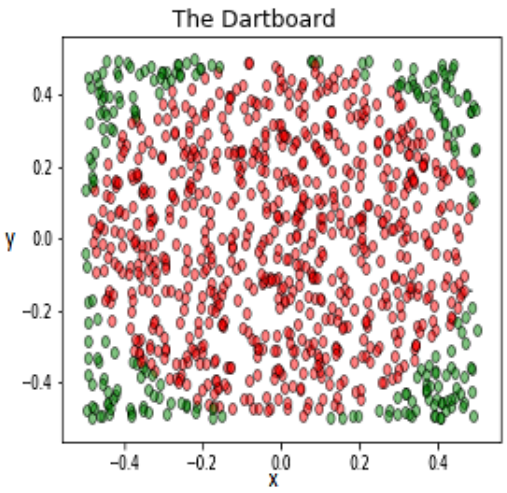

Figure 2: Darts Game Simulation

Using a probabilistic approach, the given ratio can be used to estimate the value of π as follows:

$$f = \frac{N_{circle}}{N_{square}} = \frac{Area_{Circle}}{Area_{Square}} = \frac{\pi r^2}{4r^2} = \frac{\pi}{4} \quad (1)$$

We can simulate the dart game using a random number generator code on our computer and get the value of pi. Fig. (2) shows the random points in one such simulation. Similarly, the value of other constants [4] can be estimated.

As depicted in Fig.(3), when we have fewer numbers of points, our estimates vary much more wildly and are much deviated from 3.1415926. However, the guesses from our different runs are all seen to be equally distributed around the correct value, thereby, minimising the chances of any systematic error in our estimate.

In the given simulation, the points required are randomly generated within a defined region. *This approach is the Monte Carlo Direct Sampling method, wherein, random values are generated without any history of the last value/values*. New values are generated independently and are accepted within an allowed area/region.

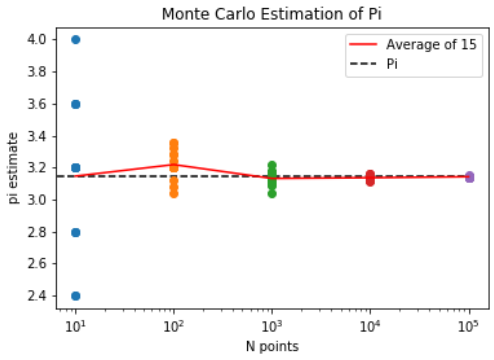

Figure 3: Monte Carlo Estimate of π

2.3 Markov chain Monte Carlo and Metropolis Algorithm:

Markov Chain Monte Carlo is a sampling method in which the generation of a new random number is governed by a previously generated random value. The parameters responsible for the new value are randomly generated, which are then added to or subtracted from the last value. This sampling method can also be understood by reconsidering the example of estimating the value of π by the dart game **with a twist**.

Imagine the dart board to be a very big playground and a person standing on it is throwing darts as javelin in random directions as depicted in Fig.(4) through Fig.(8).

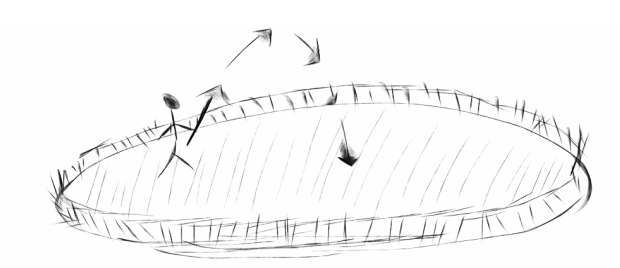

Figure 4: Dart Game with a twist

He first stands at a randomly chosen position on the playground and throws a javelin in a completely random direction. Next, he walks to the location where the javelin fell and throws another javelin in a completely random direction from this new position.If the javelin falls out of the region boundary, he continues to stand on the current position and throws a javelin again in completely random direction.

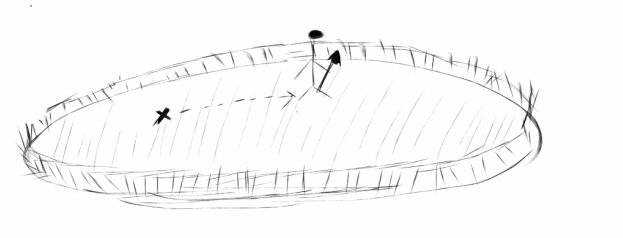

Figure 5: Throw the javelin and occupy the new position for the next throw

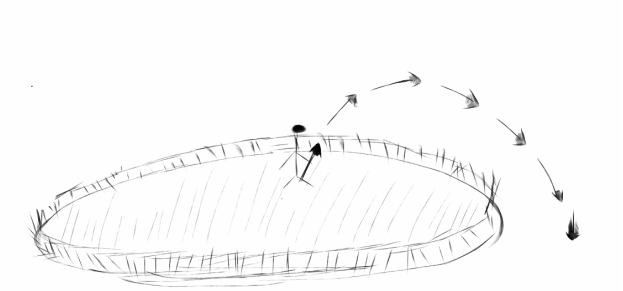

Figure 6: If the javelin is outside the ground, re-throw the javelin from the same position.

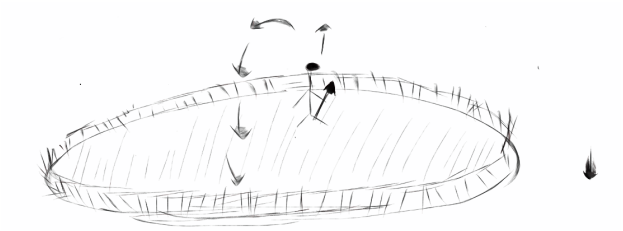

Figure 7: If the javelin is inside the ground, occupy the new position for the next throw.

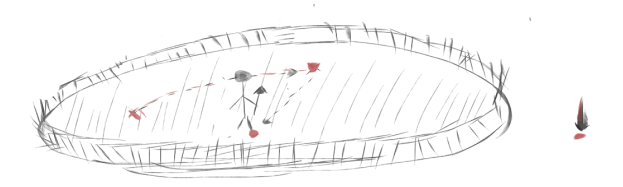

Figure 8: Sampling of the board/ground is shown as red dots

Using the described method, we sample the entire board/ground by generating a random walk [1] of points $(x_1, x_2, ...x_n)$ and hence estimate the value of π.

The Markov Chain sample asymptotically converges to the desired probability distribution, say $\pi(x)$, whereas, in direct sampling there is a direct access to $\pi(x)$. Consider the case of a random walker whose position is x_i, where i is the step of the Markov Chain Sampling. Let Δ be the randomly chosen difference between x_i & x_{i+1}. The acceptance of Δ to generate x_{i+1} is determined by the value of a parameter ω, defined as

$$w = \frac{\pi(x_{i+1})}{\pi(x_i)} \tag{2}$$

If $w \geq 1$, we accept the change and let $x_{i+1} = x_i + \Delta$, otherwise, $x_{i+1} = x_i$ and the above process is repeated.

2.3.1 Evaluation of Integrals:

The Monte Carlo method can also be used to compute integrals as explained below [5]. Let the integral to be computed be:

$$\int_0^1 h(x)dx \tag{3}$$

A large number of sample points say, $x_1, x_2, x_3..., x_n$ are chosen randomly from a uniform distribution in the range (0,1). The function $h(x)$ is computed at these points to yield a set of values $h(x_1), h(x_2)...h(x_n)$. The mean $\langle h(x) \rangle$ of these values is the computed integral value.

This method works since uniform random variables have a special property that their integral is unity over the uniform range of bound i.e. (0,1).

$$\int_0^1 f(x)dx = 1 \tag{4}$$

Now, for any function $h(x)$ if $f(x)$ is the uniform distribution, then using equation (4) we get,

$$\langle h(x) \rangle = \int_0^1 h(x)f(x)dx = \int_0^1 h(x)dx \tag{5}$$

or,

$$\langle h(x) \rangle = \frac{1}{N} \sum_{i=0}^{N-1} h(x_i) \tag{6}$$

where, N represents the sample size.

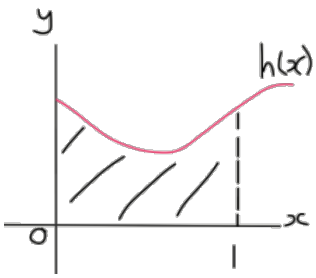

Figure 9: An example of function h(x).

Hence, we are able to compute definite integral by finding a sample mean.

2.3.2 Generalization of Evaluation of Integral for Arbitrary PDF

The formula given in equation (6) works only if the PDF (Probability Distribution function) of the random variable X is uniform. We can extend Monte Carlo integration to random variables with arbitrary PDFs. The more generic formula is given by

$$\langle h \rangle = \frac{1}{N} \sum_{i=0}^{N-1} \frac{h(X_i)}{pdf(X_i)} \tag{7}$$

The generalized expression in equation (7) can be used to solve Quantum Mechanical systems. Before diving into the actual problem solving, we need to understand the concept of Quantum Monte Carlo.

3 Quantum Monte Carlo

Most quantum mechanical problems of interest consist of a large number of interacting electrons and ions or nucleons. The total number of particles (N) is usually large and an exact solution cannot be found easily. In quantum mechanics, we can express the expectation value of a given operator $\langle \hat{O} \rangle$ for a system of N particles by equation (8), where Ψ is the wave function describing a many-body system.

For a multidimensional integral as in equation (8), the Monte Carlo methods are ideal for obtaining expectation values of quantum mechanical operators [6]. Now, our problem is that we do not know the exact wave function Ψ. So, we would invoke the concept of quantum mechanical Variational Principle in to generate a trial wave function and then attempt to perform a variational calculation of the various observables, using Monte Carlo methods.

$$\langle \hat{O} \rangle = \frac{\int dr_1 dr_2 ... dr_N \Psi^*(r_1, r_2, ..., r_N) \hat{O}(r_1, r_2, ..., r_N) \Psi(r_1, r_2, ..., r_N)}{\int dr_1 dr_2 ... dr_N \Psi^*(r_1, r_2, ...r_N) \Psi(r_1, r_2, ..., r_N)} \tag{8}$$

where $r_1, r_2, ..r_N$ are the generalized coordinates of Ψ

3.1 Variational Method in Quantum Mechanics:

According to the Variational Method, given any normalized function Ψ (that satisfies the appropriate boundary conditions), the expectation value of the Hamiltonian represents an upper bound to the exact ground state energy.[7]

$$E_o \leq \langle \hat{H} \rangle, \tag{9}$$

where, E_o is the ground state energy.

For a brief illustration of the method, let us find the ground state energy of one-dimensional harmonic oscillator, whose Hamiltonian is given by:

$$H = -\frac{\hbar^2}{2m}\frac{d^2}{dx^2} + \frac{1}{2}m\omega^2 x^2 \tag{10}$$

where, ω, m are the angular frequency and mass of the oscillator respectively. As a trial wave function, we pick a function that satisfies the boundary condition of the exact ground state wave function. The boundary condition is that the wave function vanishes at positive and negative infinities. Hence, we choose the trial wave function as,

$$\Psi = Ae^{-\alpha x^2} \tag{11}$$

where, α is the variational parameter and A is the normalization constant.

We now introduce,

$$\langle \hat{H} \rangle = \langle \hat{T} \rangle + \langle \hat{V} \rangle \tag{12}$$

where, $\hat{T}$ and $\hat{V}$ are the Kinetic Energy and Potential energy operators respectively, defined as,

$$\hat{T} = -\frac{\hbar^2}{2m}\frac{d^2}{dx^2} \tag{13}$$

giving the expectation value of kinetic energy as,

$$\langle \hat{T} \rangle = \int \Psi^* \hat{T} \Psi dx = \frac{\hbar^2 \alpha}{2m} \tag{14}$$

and

$$\hat{V} = +\frac{1}{2} m\omega^2 x^2 \tag{15}$$

giving

$$\langle \hat{V} \rangle = \int \Psi^* \hat{V} \Psi dx = \frac{m\omega^2}{8\alpha} \tag{16}$$

as the expectation value of potential energy. Minimizing the Hamiltonian with respect to the parameter alpha(α), we get,

$$\frac{d}{d\alpha}\langle \hat{H} \rangle = 0 \implies \alpha = \frac{m\omega}{2\hbar} \tag{17}$$

Using the above value of α, we get,

$$\langle \hat{H} \rangle_{min} = \frac{1}{2}\hbar\omega \tag{18}$$

as the exact ground state energy.

Having briefly discussed the Variational Principle, we now look back at Quantum Monte Carlo using the Variational Principle.

3.2 Quantum Variational Monte Carlo:

Given a Hamiltonian H and a trial wave function $\Psi(r)$, the variational principle states that the expectation value of $\langle H \rangle$ is

$$\langle \hat{H} \rangle = \frac{\int dr \Psi^*(r) \hat{H}(r) \Psi(r)}{\int dr \Psi^*(r) \Psi(r)} \tag{19}$$

Thereafter, we vary α (variational parameter) according to some minimization algorithm to find the best upper bound to the ground-state energy.

Now, having all the computational tools required to solve a quantum system, we proceed in Section B to solve a Bosonic system in a 1-D Harmonic trap.

4 Section B

4.1 Problem Statement: Bosons in 1-D Harmonic Trap

A class of particles which follows the Bose-Einstein statistics are classified as Bosons. This concept was first proposed by Satyendra Nath Bose, as an attempt to tackle the limitation of the Maxwell-Boltzmann distribution for the microscopic particles at all scales. Along with Albert Einstein, the duo developed a new statistics, now known as the Bose-Einstein statistics. This statistics governs the behaviour of non-interacting, indistinguishable particles with integral value of spins. *Such particles are known to have symmetrical wave functions.*

In this paper, we have chosen a Boson system with a large number of particles under the influence of a 1-dimensional har-

monic potential. In other words, we consider a Boson gas with N particles trapped inside a 1-Dimensional Harmonic potential well. The problem is to determine the energy eigen values of the trapped gas using the Monte Carlo Direct sampling approach and Markov-Chain sampling method. The Monte Carlo method results are then compared with the analytically obtained value.

Even though the given problem of a bosonic system is a standard one with a closed form solution, the concept of Monte Carlo sampling can be very well explained with it. There are various systems wherein the trapping potential [8] is much more complicated and the Monte Carlo method works very well for those systems.

4.2 The System, Wavefunction, Potential and Hamiltonian:

We consider N Bosons with mass m, under the influence of 1-Dimensional Harmonic Potential. Since the system is non-interacting, the internal potential is not taken into account.

The 1-Dimensional Harmonic potential is given by,

$$V(x) = \frac{1}{2}m\omega^2 x^2 \tag{20}$$

where, $\omega = \sqrt{\frac{k}{m}}$ and k is the force constant characterizing the given harmonic potential. The analytically obtained wave function of the particles under the influence of such a potential is given by [7]:

$$\Psi_n(x) = (\frac{m\omega}{\pi\hbar})^{1/4}\frac{1}{\sqrt{2^n n!}}H_n(x)e^{-x^2/2} \tag{21}$$

where the integer n labels the different energy states. The functions $H_n(x)$ are known as Hermite Polynomials. The ground state (n=0) wave function is given by,

$$\Psi_0(x) = (\frac{m\omega}{\pi\hbar})^{1/4}e^{-x^2/2} \tag{22}$$

and is depicted in Fig. (10).

Wavefunction.png

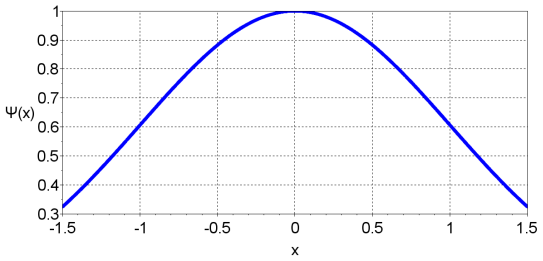

Figure 10: Harmonic Wavefunction for ground state (n=0)

Alternatively, a trail wave function can also be obtained using the concept of Variational Monte Carlo Method (Section 3.2). Accordingly, the expectation value of the Hamiltonian [6] is given by:

$$\langle\hat{H}\rangle = \frac{\int dr_1...dr_N\psi_n^*\psi_n(\frac{\hat{H}\psi_n}{\psi_n})}{\int dr_1...dr_N\psi_n^*\psi_n} \tag{23}$$

The general form of equation (23) has already been discussed in the section 2.3.2. Since we are working with discrete system of random points, the finite energy is calculated in the local region of each random point selected. So, we need to convert equation (23) to discrete form as follows:
A set of M particle configurations, $\pi_1, \pi_2, ...\pi_M$ is considered which corresponds to probability distribution $|\Psi_n|^2$.

The equivalent discrete equation can be shown to be,

$$\langle \hat{H} \rangle > \sim \frac{1}{M} \sum_{n=1}^{M} \left(\frac{\hat{H}(\pi_n)\Psi_n(\pi_n)}{\Psi_n(\pi_n)} \right) \quad (24)$$

Next, the above equation is solved by choosing some random sample using the Monte Carlo direct sampling technique and also by using the Metropolis Random Walk algorithm.

5 Evaluation of Ground State Energy Eigenvalue

5.1 Analytical Treatment

The energy eigenvalues of the particles under the influence of harmonic potential is given by,

$$E_n = (n + 1/2)\hbar\omega \quad (25)$$

where, n=0,1,2..... . Taking $\hbar = 1$ and $\omega = 1$, the ground state energy of the particles is determined to be, $E_0 = 0.5$ eV.

5.2 Monte Carlo Direct Sampling method

Now, we will apply the Monte Carlo method to compute the energy of particles inside the 1-D harmonic trap. In the equation (24), the Hamiltonian of our system is,

$$\hat{H}(x) = \frac{-\hbar^2}{2m}\frac{d^2}{dx^2} + \frac{m\omega^2 x^2}{2} \quad (26)$$

Taking $\hbar = 1, m = 1$ and $\omega = 1$ we have,

$$\hat{H}(x) = \frac{-d^2}{dx^2} + \frac{x^2}{2} \quad (27)$$

In order to calculate the expectation value of $\hat{H}$ given by equation (27), we need to consider a function Y, defined as,

$$Y(x) = \frac{\hat{H}(x)\Psi(x)}{\Psi(x)} \quad (28)$$

Using $\Psi(x)$ from equation (22), we get

$$\hat{H}(x)\Psi(x) = \frac{-d^2 e^{\frac{-x^2}{2}}}{dx^2} + \frac{x^2}{2} e^{\frac{-x^2}{2}} \quad (29)$$

Using equation (28) and equation (29) we get,

$$Y(x) = 1 - \frac{x^2}{2} \quad (30)$$

The Maxima of Y(x) is given by:

$$\frac{dY(x)}{dx} = 0 \quad (31)$$

Equation (31) gives the maximum value as Y(0)=1. This is the upper limit of the energy curve. To select such a sample we first follow the Monte Carlo direct sampling method discussed in section 2.2.

The sample chosen is in the form of x_i and y_i where i runs from 1 to N. Here, x_i represents the randomly chosen position of the i^{th} particle within some arbitrary range and y_i is the corresponding energy value bounded by the upper limit of Y(x). Out of the random sample of x_i and y_i, only certain points are chosen according to the acceptability method described below:

Whenever a random value of y is generated, it is compared with the corresponding value of H(x), if $y < H(x)$, then x_i is accepted, which in turn means that the corresponding value of Hamiltonian is selected, else it is rejected.

Let the number of accepted values be p, where $p \leq N$. Using these accepted values we estimate the ground state energy of the Hamiltonian by calculating the mean of all the individual Hamiltonian values at each point. Figure (11) depicts the variation of the Hamiltonian with the randomly generated x range using the Direct Sampling Method.

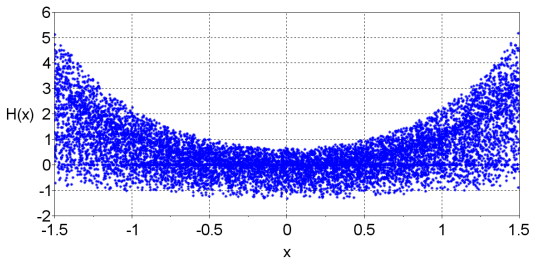

Figure 11: Variation of the Hamiltonian with the randomly generated x range using the Direct Sampling Method

The estimated ground state energy value by Direct Sampling Method (using Scilab [9]) is 0.5415408 eV.

5.3 Markov Chain Monte Carlo method : Random Walk Sampling

In Markov Chain sampling, we have used the ideas discussed in Section 2.3. Let the variable, n_{trials}, represent the number of random walks we use in the program. Initially, we choose a random value of x and y, which are subsequently updated in accordance to Markov Chain Method to generate a random path comprising of p number of accepted points. The process is repeated to generate such multiple random walks ($= n_{trials}$) to cover the entire under the given energy curve. At each of the accepted points (x, y), the value of Hamiltonian is computed and summed to give the total Hamiltonian, which is then divided by $p * n_{trials}$ to give the value of energy of Bosons. The condition of acceptability of a Hamiltonian value for a certain point is the same as discussed in the direct sampling method (Sec 5.2).

5.4 Random Walk Plots

Fig. (12) through Fig. (19) depict the plots of Y(x) and the corresponding Hamiltonians H(x) for an increasing number of random walks (n_{trials} = 1, 2, 10 & 50). The computed values of ground state energy in each case are given in table (1).

Number of Random Walks	Estimated Ground State Energy (eV)	Error(%)
1	0.1718306	65.63
2	0.902497	80.49
10	0.5768063	15.36
50	0.5690777	13.82

Table 1: Computed Values of Ground State Energy for Different Random Walks

It can be seen from the table and the random walk plots that as the number of random walks is increased, i.e., a larger portion of the area under the Y(x) energy curve is

covered, the estimated ground state energy approaches the exact value.

1. For 1 random walk

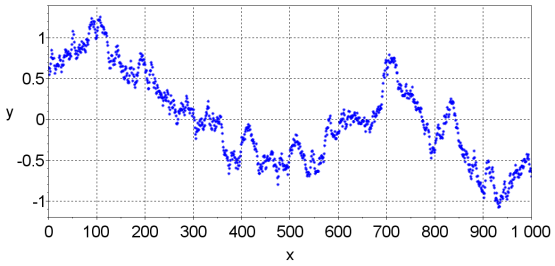

Figure 12: Random Walk-1

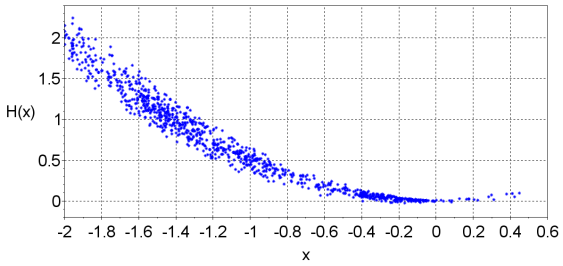

Figure 13: Hamiltonian Plot for Random Walk-1

2. For 2 random walks

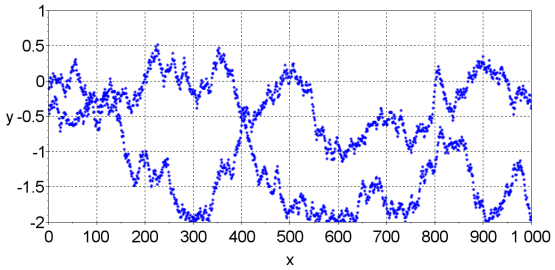

Figure 14: Random Walk-2

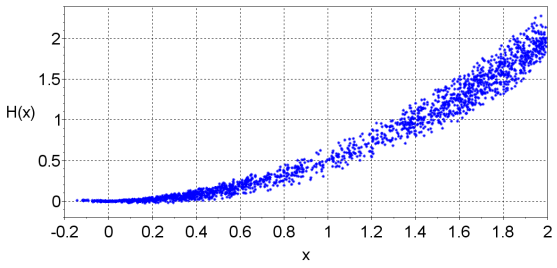

Figure 15: Hamiltonian Plot for Random Walk-2

3. For 10 random walks

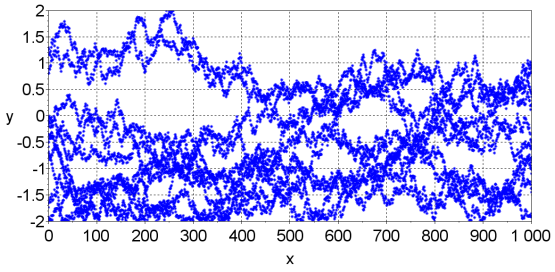

Figure 16: Random Walk-10

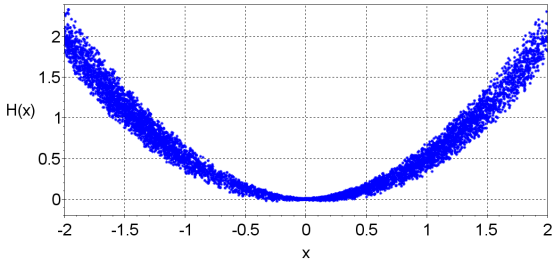

Figure 17: Hamiltonian Plot for Random Walk-10

4. For 50 random walks

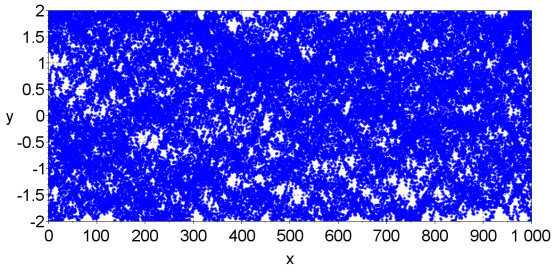

Figure 18: Random Walk-50

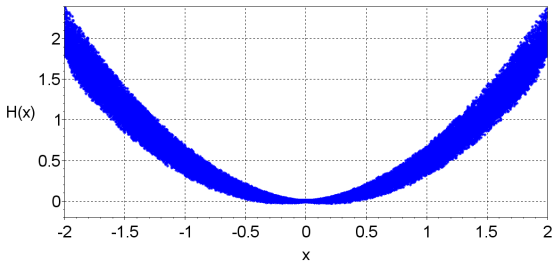

Figure 19: Hamiltonian Plot for Random Walk-50

6 Results and Discussions:

In this paper we have used the two approaches of sampling as described in Section A. We saw through this paper that Monte Carlo method gives us a strong and powerful tool, to solve the Hamiltonians to compute energy eigenvalues. It is quite an elegant concept for the potentials which are complicated and are difficult to solve analytically. Monte Carlo equips us to solve such complicated potentials without getting into tedious mathematics, where chances of er-

rors are more.

The computation of ground state energy of Bosonic gas under the influence of 1-D Harmonic potential using the Monte Carlo direct sampling method and the Metropolis method yielded results in good agreement with the exact value of 0.5 eV.

References

[1] Werner Krauth. Statistical mechanics: algorithms and computations. Oxford University Press, 2012.

[2] David P. Landau. The metropolis monte carlo method in statistical physics. In AIP Conference Proceedings. AIP, 2003.

[3] D. E. Raeside. An introduction to monte carlo methods. American Journal of Physics,42(1): 2026, January 1974.

[4] Pirooz Mohazzabi. Monte carlo estimations of e. American Journal of Physics, 66(2): 138140, February 1998.

[5] S Iskandar. Modified monte carlo method for integral. Journal of Physics: Conference Series, 1462 : 012061, February 2020.

[6] J. L. DuBois and H. R. Glyde. Bose-einstein condensation in trapped bosons: A variational monte carlo analysis. Physical Review A, 63(2), January 2001.

[7] David Griffiths. Introduction of Quantum Mechanics. Prentice Hall, Inc., 1995.

[8] Salvio Jacob Bereta, Lucas Madeira, Vanderlei S. Bagnato, and Monica A. Caracanhas. Boseeinstein condensation in spherically symmetric traps. American Journal of Physics,87(11): 924934, November 2019.

[9]]S. Enterprises, Home - Scilab, Scilab.org, 2017. [Online]. Available: https://www.scilab.org/

New and simple method for the determination of critical damping resistance of moving coil galvanometer

Bhakta Kunwar

Post –Graduate Department of Physics, Sikkim Government College,
Tadong, Gangtok, Sikkim, India-737102.

E-mail: bhaktakunwar@yahoo.co.in

Submitted on 25-02-2021

Abstract

Moving coil galvanometer is one of the most frequently used apparatus in electromagnetic measurements of any undergraduate physics laboratory. The critical damping resistance of a moving coil galvanometer is a crucial parameter for determining its operation either as a dead beat galvanometer or as a ballistic galvanometer. The value of critical damping resistance is provided in the data sheet by some of the standard manufacturers of galvanometer. Ironically, many of the manufacturers do not provide it. Methods of measuring critical damping resistance in a laboratory have been discussed by few authors. However, these methods are meticulous, involved and time consuming from the point of view of a student working within a limited time in a laboratory. In this paper we present a simple and alternate method of determining critical damping resistance of a moving coil galvanometer. Firstly, we present the theory concerned and derive the required working formula. No approximations have been made in the underlying theory while deriving the working formulae. Then, we illustrate the method by performing an experiment. The method is simple and less time consuming.

1. Introduction

A moving coil galvanometer (MCG) is used in a variety of electromagnetic measurements in an undergraduate physics laboratory. It not only offers scope to understand basic interactions in electricity and magnetism but also finds applications in various sensitive measurements. As is well known, an MCG can be used either as dead beat galvanometer or as a ballistic galvanometer (BG). A dead beat galvanometer can measure steady current while a BG can measure a momentary flow of charge.

An MCG can be made to operate in BG mode simply by connecting an external resistance, having a value greater than the so called 'critical damping resistance' (CDR), in series with the galvanometer. An MCG function as a dead beat galvanometer if the external resistance is less than the CDR. The theory of MCG, its construction and design were well known by the beginning of twentieth century [1,2,3,4]. Some of the MCGs are designed to operate in critically damped conditions, the theory and method of designing such MCGs can be found in the literatures, for example in [5]. The value of CDR of a given MCG depends on intrinsic constants of the materials used in its construction such as moment of inertia

of suspended coil, restoring constant of suspension, magnetic field, and area and number of loops in the coil. Methods of measuring CDR of a general MCG in a laboratory have been discussed by several authors [6,7]. These methods are meticulous, involved and time consuming from the point of view of an undergraduate student working within a limited time in a laboratory. We present a simple method of finding CDR in a laboratory by using simple formulae which have been derived without involving too many approximations. The method and the formulae have been tested and verified through experimental investigations.

In the following sections, we briefly describe construction and theory of MCG. Subsequently, we derive a working formula for finding CDR and we describe the procedure for performing the proposed experiment. Finally we illustrate our proposition with experimental data.

2. Construction and theory of the galvanometer

An MCG consists of a movable coil suspended in the magnetic field of permanent magnet. When an electric current is passed through the coil, the latter experiences a torque due to the Lorentz force. The torque rotates the coil until the driving torque is balanced by the restoring torque of the coil suspension. Let N be the number of turns in the coil, A be the area of coil and B be the strength of magnetic field. Let us introduce a constant, $G = NAB$.

If I is the moment of inertia of suspended coil about its axis of rotation, a is the damping constant due to air etc., c is restoring constant, θ is the angle of deflection of the coil after time t of applying a dc emf E to the galvanometer circuit as shown in figure 1, then the equation of motion of the moving system is

$$I\frac{d^2\theta}{dt^2} + a\frac{d\theta}{dt} + c\theta = \frac{G}{R}\left(E - G\frac{d\theta}{dt}\right), \qquad (1)$$

where R, the total resistance of the circuit, is given by $R = R_g + R_e$, R_g and R_e being the resistances of MCG and the external resistance respectively. The equation of motion of the coil can be written as

$$\frac{d^2\theta}{dt^2} + 2p\frac{d\theta}{dt} + q^2\theta = f, \qquad (2)$$

where $$p = \left(\frac{a}{2I} + \frac{G^2}{2IR}\right), \qquad (3)$$

$$q = \sqrt{\frac{c}{I}}, \qquad (4)$$

and $$f = \frac{GE}{IR}. \qquad (5)$$

The behavior of MCG will be overdamped, critically damped or underdamped according as $p^2 > q^2$, $p^2 = q^2$ or $p^2 < q^2$ respectively. In the underdamped condition, that is when $p^2 < q^2$, the motion of the coil is oscillatory and its amplitude is given by

$$\theta = \theta_0\{1 - Ae^{-pt}sin(\omega t + \alpha)\}, \qquad (6)$$

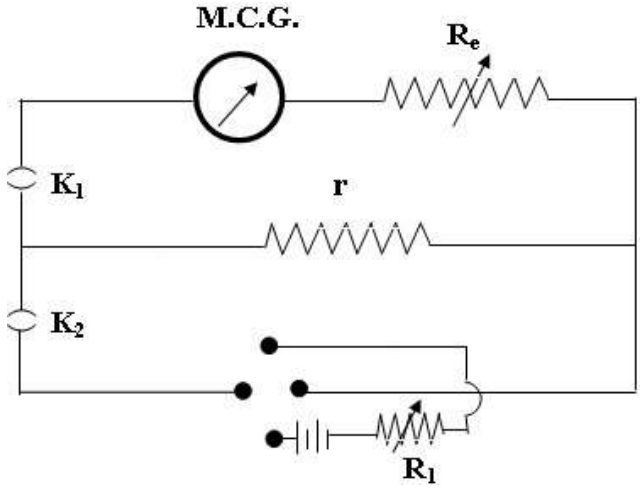

Figure 1. Circuit diagram for the determination of critical damping resistance of an MCG. Low resistance r is used for providing a potential difference across MCG via external resistance R_e. Variable resistance R_1 in the battery circuit is

used for adjusting the emf so as to produce ballistic throw within the scale.

where ω is the angular frequency and is given by $\omega = \sqrt{q^2 - p^2}$. The constants A and α in eq.(6) are given by $A = \sqrt{(p^2/\omega^2) + 1}$ and $\alpha = tan^{-1}(\omega/p)$.

The time period of oscillation $T = 2\pi/\omega$ can be expressed as

$$T = \frac{2\pi}{\sqrt{\frac{c}{I} - \frac{(a+G^2/R)^2}{4I^2}}}. \qquad (7)$$

The eq.(6) represents a damped oscillation about the final steady deflection θ_0.

2.1 About Damped Oscillation

If an MCG is made to operate in underdamped condition and a current is passed through it by inserting both the keys K_1 and K_2 in their positions as shown in figure 1, the coil would undergo oscillatory motion about a mean position. The coil would finally reach a steady state with steady deflection θ_0 .The amplitudes of moving system under this condition are given by eq.(6).
Now, if K_2 is suddenly removed from the circuit keeping K_1 fixed in its position, the coil would undergo damped oscillation about its equilibrium position (zero position of scale) and the variation of θ with time t is then given by

$$\theta = \theta_0 e^{-pt} sin\omega t. \qquad (8)$$

If θ_1 be the first peak throw on one side of the zero, θ_2 the second throw on the other side, θ_3 the third throw (on the side of θ_1), θ_4 the fourth peak throw (on the side of θ_2) and so on. Then,

$$\frac{\theta_1}{\theta_2} = \frac{\theta_2}{\theta_3} = \frac{\theta_3}{\theta_4} = \cdots = e^{pT/2} = x\,.$$

The quantity $\ln x$ is called logarithmic decrement and is denoted by λ as

$$\lambda = \ln x = \frac{pT}{2}\,. \qquad (9)$$

In order to eliminate the individual errors introduced by inaccurate readings due to shifts of the zero of the scale, log decrement λ can be obtained from the relation

$$\lambda = \frac{1}{2n} ln \frac{\beta_1}{\beta_{2n+1}} \qquad (10)$$

where $\beta_1 = \theta_1 + \theta_2$, $\beta_2 = \theta_2 + \theta_3$ and so on. Since $\beta's$ are the sum of the successive deflections on the two sides of the zero of the scale, the errors affecting the individual deflections due to the inaccurate reading of zero are eliminated. See textbook such as Feweks and Yarwood [8].

3. Our proposition: Working Formula and experimental procedure

For a given value of external resistance R_e, one can achieve steady state with both the keys K_1 and K_2 fixed in their positions. Then, if K_2 is suddenly removed from the circuit keeping K_1 fixed, the coil would undergo damped oscillation about the zero position as discussed above. Then one can measure and record the values of θ_1, θ_2, θ_3, etc. and from these measured values of deflections one can find logarithmic decrement λ using eq.(10). One should also measure time period T at this value of R_e. After measuring λ and T for this value of external resistance R_e, we can find the damping term p from eq.(9). Next, we change the values of R_e and repeat the above procedure so as to obtain λ , T and p at different values of R_e. We also find values of λ, T and p at $R_e = \infty$; this is done by taking out both the keys K_1 and K_2 from their positions after achieving steady state. Such oscillations are usually called the open circuit oscillations. If we plot a graph with reciprocal of R along x-axis and p along y-axis, then, we should get a straight line according to eq.(3). The slope of this straight line should be equal to $G^2/2I$ and the intercept on y-axis should give the value of $a/2I$.

Moreover, in the open circuit oscillations, $R_e \rightarrow \infty$ and therefore, $R \rightarrow \infty$. This implies from eq.(3) that the experimentally obtained value of in the open circuit condition, say p_∞, must also be equal to $a/2I$. So, it is expected that the intercept on y-axis should match with measured value of p_∞.

Now, one can derive from eqs(3) and (7)

$$\frac{c}{I} = p^2 + \frac{4\pi^2}{T^2} \qquad (11)$$

Using the the values of T and p measured at different values of R_e, one can find the values of c/I at corresponding values of R_e from eq.(11). Consequently, an average value, say $(c/I)_{av}$, can be obtained from the above set of values of c/I calculated at different R_e. But, as c and I both are intrinsic constants for a given MCG, the value of c/I and hence the right hand side of eq.(11) should also be a constant. It is worth mentioning here that values of T and p measured in open circuit condition have the lowest error and therefore the value of c/I calculated with these values of T and p is expected to be close to the average value $(c/I)_{av}$.

Now, the condition for critical damping is $p^2 = q^2$. Let this condition be achieved at $R_e = R_{cdr}$; this R_{cdr} is termed as critical damping resistance (CDR). The condition $p^2 = q^2$ can also be expressed as

$$\left\{\frac{a}{2I} + \frac{G^2}{2I(R_g + R_{cdr})}\right\}^2 = \left(\frac{c}{I}\right)_{av}, \qquad (12)$$

where we have used average value of c/I. From eq.(12), one can easily find an expression for critical damping resistance R_{cdr} as

$$R_{cdr} = \frac{G^2/_{2I}}{\sqrt{\left(\frac{c}{I}\right)_{av}} - \frac{a}{2I}} - R_g \qquad (13)$$

The values of terms $G^2/2I$ and $a/2I$ on the right hand side of eq.(13) are obtained from the slope and intercept of the straight line drawn with $1/R$ along x-axis and p along y-axis, while $(c/I)_{av}$ is calculated from eq.(11) as discussed above. Thus, knowing values of T and p at different values of R_e, one can find the value of critical damping resistance R_{cdr} of a given MCG under a given operational condition.

4. Experimental data and results

We present here an experimental data which was carried out hurriedly for the verification of the proposed theory as a first time check. As such, the experimental data and the results eare mainly aimed for illustrative purpose. We took an MCG (Besto India made with R_g= 200 Ω) and made connections as shown in figure 1. Then, we adjusted the Variable resistance R_1 and the value of low resistance r so as to produce ballistic throw within the scale. For R_e= 2 kΩ to 18 kΩ, the supply dc voltage (emf) was maintained at 16.2 V. This voltage was changed during measurements at R_e= 20 kΩ and at R_e= ∞. These changes in voltage was done so as to obtain noticeable deflection in the scale (see Table 1: the deflections at R_e= 20 kΩ and at R_e= ∞, marked * in Table 1, are not in proportion to the deflections at R_e= 2 kΩ to 18 kΩ). Such adustments in voltage does not affect the values of T and p as these quantities depend on external resistance R_e and other intrinsic constants of the galvanometer. However, low resistance r and other operational conditions remain the same throughout the experiment. We chose r = 0.01Ω. Deflections of the galvanometer were measured for different values of external resistance R_e following the procedure described in the previous sections and are presented in Table 1.

The readings are taken in cm from the linear scale. Obviously, these linear readings are proportional to the angular deflections of the coil.

The values of log decrements $\boldsymbol{\lambda}$ at each resistance were calculated using eq.(10) and then damping terms $\boldsymbol{p}$ were obtained using eq.(9). Thereafter, values of $\boldsymbol{c/I}$ were found from eq. (11). The values of $\boldsymbol{T}$, $\boldsymbol{\lambda}$, $\boldsymbol{p}$ and $\boldsymbol{c/I}$ for each resistance $\boldsymbol{R_e}$ are presented in Table 2. The error in the measurement of $\boldsymbol{\lambda}$ at $\boldsymbol{R_e}$= 2 kΩ was about 24% and hence it was ignored for further calculations. Errors in the individual measurements of $\boldsymbol{\lambda}$ for $\boldsymbol{R_e}$= 3 kΩ and above was well below 10 %.

On plotting a graph with $\boldsymbol{1/R}$ along x-axis and $\boldsymbol{p}$ along y-axis we obtained a straight line as shown in figure 2. From this graph we obtained slope, $\boldsymbol{G^2/2I}$ = 356 ± 12 Ω and intercept, $\boldsymbol{a/2I}$ = 0.006 ±0.002 (linear fit R^2 = 0.9955). The average value of $\boldsymbol{c/I}$, that is $\boldsymbol{(c/I)_{av}}$, was found to be 0.123 ±0.002. As expected, value of $\boldsymbol{c/I}$ in the open circuit condition is 0.123. Finally, critical damping resistance was obtained by using eq.(13). The experimentally measured value of critical damping resistance ($\boldsymbol{R_{cdr}}$) was found to be 833±49 Ω.

Table 1. Experimental data showing galvanometer deflections at different values of external resistances.

Resistance R_e (kΩ)	Time period T (s)	1st Throw θ_1 (cm)	θ_2 (cm)	θ_3 (cm)	θ_4 (cm)	θ_5 (cm)	θ_6 (cm)	θ_7 (cm)	θ_8 (cm)	θ_9 (cm)	θ_{10} (cm)	θ_{11} (cm)	θ_{12} (cm)
2	20.7	12.3	2.1	0.4	0.1								
3	19.2	9.9	3.1	1.2	0.2								
4	18.9	8.3	3.5	1.6	0.6	0.4							
6	18.3	6.4	3.6	2.2	1.1	0.7	0.3						
8	18.2	5.5	3.5	2.4	1.4	1	0.5						
10	18.1	4.8	3.4	2.4	1.6	1.2	0.8	0.5	0.4				
12	18	4.5	3.3	2.5	1.7	1.3	0.9	0.7	0.4				
14	18	4.3	3.3	2.6	1.9	1.5	1.1	0.9	0.6	0.5			
16	17.9	3.1	2.5	2	1.5	1.3	0.9	0.8	0.5	0.4			
18	17.9	3	2.4	2	1.5	1.3	1	0.8	0.6	0.5	0.4		
20	17.9	8.5*	6.7	5.6	4.5	3.7	2.9	2.5	1.9	1.6	1.3	1.1	0.8
Open	17.9	11.8*	11.4	10.7	10.3	9.7	9.4	8.7	8.5	8	7.7	7.2	7

Table 2. The values of Time period ($\boldsymbol{T}$), log decrement ($\boldsymbol{\lambda}$), damping term ($\boldsymbol{p}$) and $\boldsymbol{c/I}$ for each resistance R_e.

Resistance R_e(Ω)	Time period T(s)	Log decrement λ	Damping term p	c/I
2000	20.7	1.68	0.16	-
3000	19.2	1.11	0.12	0.122
4000	18.9	0.84	0.09	0.119
6000	18.3	0.58	0.06	0.122

8000	18.2	0.45	0.05	0.122
10000	18.1	0.37	0.04	0.122
12000	18.0	0.33	0.04	0.124
14000	18.0	0.27	0.03	0.123
16000	17.9	0.24	0.03	0.124
18000	17.9	0.22	0.03	0.124
20000	17.9	0.21	0.02	0.124
Open	17.9	0.05	0.01	0.122

Figure 2. A plot with $\boldsymbol{1/R}$ along x-axis and $\boldsymbol{p}$ along y-axis showing the variation of damping term p with external resistance $\boldsymbol{R_e}$. It is to be noted that the total resistance $\boldsymbol{R = R_g + R_e}$, where $\boldsymbol{R_g}$ is galvanometer resistance. The black solid points denote experimental data while the red coloured straight line is a linear fit.

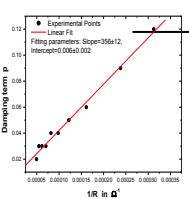

5. Discussion

Even though most of the standard manufacturers of MCG provide the value of R_{cdr} , there are many manufacturers which provide no other data except the resistance of the Galvanometer. In such scenario it becomes important for the student to have, at least, a rough idea about the value of R_{cdr} so that the set up could be used as a BG. The method of finding critical damping resistance of an MCG presented in this paper is simple, straightforward and less time consuming. The working formulae used in this method have been analytically derived without making any approximations. In the illustrative experiment presented in this paper we have started our data from R_e = 2000 Ω onwards. At 2000 Ω, the coil makes only two oscillations before it comes to equilibrium position and the relative error here is about 0.25, hence this data was ignored for the calculations. We have only considered experimental data corresponding to R_e >2000 Ω for further calculations. We also observed that the value of *c/I* can be directly evaluated by substituting the values of *p* and *T* corresponding to open circuit in eq.(11). This way one can do away with the lengthy process of finding average value of *c/I* . The difference in values of *c*/*I* obtained from these two different technique is almost negligible. Although the number of oscillations made by the coil before it comes to rest at equilibrium position may be fewer at lower values of external resistance R_e it is advisable to include these readings as the variation of time period and logarithmic decrements are prominently seen at lower resistances. Besides knowing the value of CDR this method also gives an idea about the relative values of , and . The overall accuracy in the determination of the value of R_{cdr} in this experiment is within 5 %. The main focus of the present work is the presentation of the working formula and methodology. The experimental part has been included in the present work primarily to give a fillip to the understanding of the underlying theory and procedure.

References:

[1]O.M. Stewart, The Damped Ballistic Galvanometer, Phys. Rev. 16,158(1903)

[2]W. P. White, Sensitive Moving Coil Galvanometers, Phys. Rev. 19, 305(1904)

[3]W. Jaeger, Über das Drehspulengalvanometer, Annalen der Physik 326, 64(1906)

[4]W. P. White, Every-day Problems of the Moving Coil Galvanometer, Phys. Rev. 23, 382(1906)

[5]F. Wenner, General Design of Critically Damped Galvanometers, Bulletin of the Bureau of Standards 13, 211(1916)

[6]R. N. Rai, Moving Coil Galvanometer and Critical Damping, American Journal of Physics 12, 151 (1944);

[7] G. W. Rodeback, The Moving Coil Ballistic Galvanometer Revisited, Rev. Sci. Instrum. 43, 837 (1972)

[8]Feweks J.H. and Yarwood J. *Electricity and Magnetism Volume I,* University Tutorial Press Ltd., London,1965

Novel method for determination of contact angle of highly volatile liquids

V Madhurima and K Nilavarasi

Department of Physics,
Central University of Tamil Nadu,
India-620015.

nilavarasikv@gmail.com

Submitted on 07-09-2021

Abstract

In this paper, a novel method for the measurement of equilibrium contact angle of highly volatile binary liquids is proposed. The proposed computational method, which combines finite element method and energy equilibration, calculates the solid-liquid contact area, which can then be used to estimate the equilibrium contact angle. Using the proposed approach, the contact angles of binary-liquid droplet on a microgrooved and smooth polycarbonate substrate were calculated. The proposed method is found to be an efficient tool for finding the contact angle of all liquids (both volatile and non-volatile).

1 Introduction

Wettability becomes crucial for many industrial and scientific applications such as painting/coating [1, 2, 3, 4], surface chemistry [5], oil recovery [1, 2, 3, 4] and so on. Wettability describes the balance of three inter-facial interactions namely, solid-liquid (γ_{sl}), liquid-vapor (γ_{lv})and solid-vapor (γ_{sv}) inter-facial interactions [6, 7, 8]. The balance between such three interactions are expressed by Young's equation [9, 10, 11],

$$\gamma_{lv} cos\theta = \gamma_{sv} - \gamma_{sl} \tag{1}$$

where θ is the contact angle. Although the surface tension of the liquid can be measured experimentally with satisfactory accuracy, the solid-liquid inter-facial tension cannot be measured directly, and therefore the wettability is usually described by the contact angle, which is the angle formed between the solid-liquid interface and the liquid-vapor interface. The contact angle is measured experimentally using the standard sessile drop method, in which the camera focuses on a liquid droplet placed over a solid substrate and the geometry of the droplet is used to obtain the contact angle [12].

Apart from sessile droplet method, there are also other methods of measuring contact

angle directly which includes ”tilting plate” method [13, 14], captive bubble method, etc., [15, 16, 17]. Although the measurement of contact angle from these methods is relatively straightforward, there are issues that require attention while using volatile liquids: 1. The inherent inaccuracy of the direct measurement techniques and 2. simultaneous variation in the contact area and contact angle of the liquid over the solid surfaces [18]. There have been numerous studies reporting contact angles for a variety of liquids, binary systems, etc., In most such studies, the liquids used are less volatile and the binary system used contains water as one of its moiety [19].

In the present paper, an attempt is made to address the problem of measuring contact angle of highly volatile liquids. Here, equilibrium droplet shape of highly volatile binary liquids on the horizontal smooth and constrained surfaces are simulated to obtain the contact angle of binary liquids on solid surfaces. This 3D-drop shape model is used to numerically analyze the shape, contact area and contact angle of the liquid droplets over the solid surface. The effect of variation of surface tension and surface roughness on the drop shape and apparent contact angle is examined. The liquids used in the present study include methanol, ethanol and different concentrations of the ethanol-methanol binary system. The simulated results are validated with the experimentally obtained data. The present study shows that the proposed method can be an efficient tool for finding the contact angle of all liquids (both volatile and non-volatile).

The contact angle measurements are also useful in determining the size of the pores formed as a result of self-assembly of condensed liquid droplets. Since, pore size is a measure of diameter of a triple phase contact line. In the present study, an attempt is also made to compare the experimental pore size of the self-assembled droplet patterns with the simulated droplet size.

2 Simulation Details

The equilibrium shape of a liquid drop is achieved through energy minimization. In the present study, the finite element method and gradient descent method is used to evolve the surface toward minimal energy using *Surace evolver* [20, 21]. In this the liquid droplet equilibration is achieved by minimizing various energies namely, surface tension, gravitational energy, etc., involved in the defined system. The initial geometrical parameters, energies and constraints involved in the system are given as inputs and the program minimizes the total energy of the system by modifying the surface geometry according to the defined parameters and constraints. The droplet size of the binary liquid obtained from simulated stable equilibrium shape of various liquid droplets over specific smooth and constrained surfaces are compared with those from experiments.

In the present work, the gravitational effect

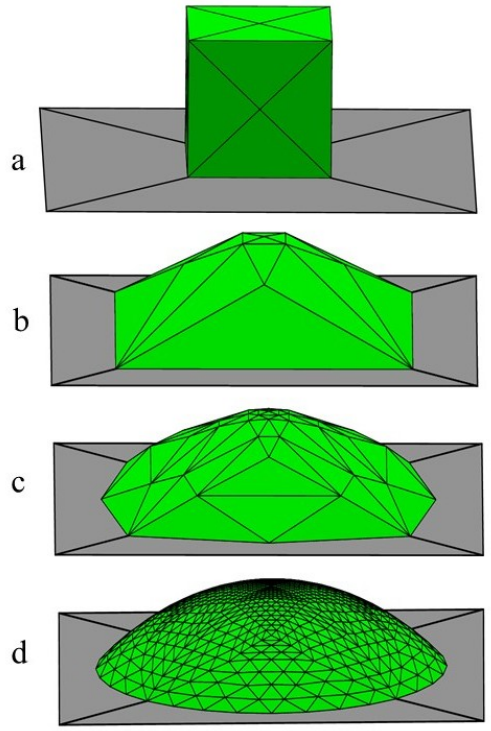

Figure 1: System evolving from initial geometry. a) Initial drop b) After 100 refinements c) After 200 refinements and d) Final shape of the droplet.

is negligible and hence do not influence the results significantly. Therefore, gravitational energy was not taken into account. The initial geometry and the shape after successive evolutions are shown in Figure 1. The free energy of the system is expressed as [22],

$$G/\gamma_{lv} = A_{lv} - \int\int \cos\theta dA \qquad (2)$$

and the contact angle (θ) is defined by Young's equation [9, 10, 11]. Here in equation 8, γ_{lv} refers to surface tension of the liquid and A_{lv} refers to the liquid-vapor contact area. The drop volume specified in this work is 9 μl. The bottom face of the droplet is constrained to move and this boundary condition is considered to be responsible for obtaining the shape of the droplets. For the sake of convenience, the constraints are specified to the edges which defines the three phase contact line. The successive refinements and steps concerning energy minimization computes the equilibrium shape of the system. Figure 1 gives the illustration of the steps involved in the *Surface Evolver* simulation.

3 Results and Discussion

3.1 Smooth surfaces

Measuring the contact angle of the highly volatile liquid is experimentally difficult [5, 15]. Hence, in the present study, *Surface Evolver* is used to model the wetting behavior of the ethanol-methanol binary liquid drop on the smooth surface. For this solid-liquid inter-facial tension calculated from experiments is used an input parameter instead of conventionally used contact angle. The variation of solid-liquid inter-facial tension for various concentration of methanol is shown in Figure 2.

The shape of the surfaces after the minimization of surface free energy are shown in Figure 3 and 4. It is observed from the figure that the variation of concentration of binary liquid affects the width and height of the liquid drops on the smooth surface. Hence the shapes calculated from *Surface Evolver* helps in understanding the variation of pores shapes with varying concentration of methanol [23].

The solid-liquid inter-facial tension for all concentration of ethanol-methanol binary sys-